Supplementary Materials and Methods

Whole-mount in situ hybridization (WISH) and immunofluorescence (IF)

Digoxigenin-labeled antisense RNA probes were synthesized by *in vitro* transcription. ISH was performed as described (Lin et al., 2005; Thisse and Thisse, 2008), and the embryos were then sectioned to 10 μm thickness, as described previously (Barthel and Raymond, 1990). Immunofluorescence (IF) staining of sections was performed as described previously (Trinh and Stainier, 2004). For vibratom sectioning, embryos were fixed in 4% PFA overnight at 4°C, embedded in 4% low-melting agarose and sectioned at 200 μm thickness using a Vibratome 1500 (Intracel). For whole-mount IF staining, embryos were fixed in 1% PFA/0.01% Triton X-100 for two hours at room temperature, and then the yolk was manually removed by gentle pipetting in PBS/0.01% Triton X-100. The deyolked embryos were re-fixed in 4% PFA overnight at 4°C.

IF staining was performed in PBDT (1%BSA, 2% goal serum, 2% DMSO, 0.1% Triton X-100 in PBS) as previously described (Ye and Lin, 2013). The following antibodies were used for immunostaining: anti-$G\alpha_{13}$ antibody (1:100, a gift from Dr. David Manning at University of Philadelphia), which recognizes both zebrafish $G\alpha_{13}$a and $G\alpha_{13}$b, as shown in our previously published study (Lin et al., 2005); anti-GFP antibody (1:200, Santa Cruz); anti-ZsYellow (1:200, Origene); anti-Kaede (1:200, MBLI); anti-ZO1 (1:200; Invitrogen); anti-Fibronectin (1:200, Sigma); anti-PKCζ (C-20, 1:200, Santa Cruz); and rabbit anti-β-catenin (1:200, Sigma).

Microscopy, time-lapse imaging and image analysis

For still epifluoresence images, live or fixed embryos were mounted in 2% methylcellulose and photographed using a Leica DMI 6000 microscope with a 5×/NA 0.15 objective. For ISH images, embryos and sections were mounted in 75% glycerol/PBS and photographed using a Leica M165FC Stereomicroscope with a Leica DFC290 Color Digital Camera or Nikon Microphot-FX microscope respectively. Confocal images were acquired using a laser-scanning confocal inverted microscope (LSM700, Carl Zeiss, Inc.) with a LD C-Apo 40×/NA 1.1 water objective unless described specifically. *Z*-stacks were generated from images taken at 0.25-0.4 μm intervals, using the following settings (1024x1024 pixel, 8 speed, 4 averaging).

For epifluoresence time-lapse imaging, the embryos were embedded in 0.8% low-melting agarose in a dorsal-mount imaging mold (Megason, 2009). The anterior region of the endoderm was

focused, and re-adjusted as necessary throughout the imaging period so that this region remained clearly visible. Time-lapse microscopy was performed at 25°C, with images taken at 5-minute intervals using an inverted Leica DMI 6000 microscope with a 5×/NA 0.15 or 10×/NA 0.3 objective. To accurately estimate the developmental stage, we chose embryos with the same somite number for agarose embedding, and recovered them from the agarose to re-evaluate the somite number after imaging was completed. The actual number of somites formed in each embryo during the time-lapse period was determined and plotted against average width of the endoderm. We found that at the end of the imaging period the *mil* mutant was 1-2 somites delay in development. The images were processed using the Metamorph software (Molecular Devices) and analyzed using ImageJ. Endoderm width was assessed at the regions where myocardial cells are populated, as indicated by the yellow lines (equivalent length for embryos at the same stage). To calculate the speed of endoderm convergence, we used the following formula: Speed (somite X) = [endoderm width at somite X – endoderm width at somite (X-1)]/minutes during which one somite developed. For example, in Fig. 2P, the speed of endoderm convergence at 14 s refers to the average velocity of the endoderm movement from 13 s to 14 s. Therefore, the endoderm reached its minimal width at 14s and stayed at approximately that width until 16 s (Fig. 2O); this is reflected by the speeds at 15-17 s, which are close to zero.

For *in toto*, high-resolution confocal imaging, embryos were embedded in 0.8% low-melting agarose in 35-mm glass-bottom petri dishes (MatTek), and were scanned using the LSM700 microscope with a LD C-Apo 40×/NA 1.1 water objective. *Z*-stack images at 1.4-μm intervals (covering all myocardial precursors and the endoderm) were acquired every 5 minutes, using the following settings: 512×512 pixels, maximum speed, two averaging and a 1.28 air unit Pinhole). The orthogonal *XZ* images for each time frame were generated using ImageJ, and were merged into a stack file. All images of the same type were acquired using the same settings, and were then edited and compiled using Adobe Photoshop and Adobe Illustrator software. For the migration of myocardial cells, confocal time-lapse was performed in *Tg(nkx2.5:lifeact-GFP)* embryos using a Lan-Apo 20×/NA 0.8 objective. *Z*-stack images were collected at 1.5-μm intervals (covering most myocardial precursors) every 35 seconds, using the following settings: pixels, 512×512; speed, 7; average, 4.

For quantification of the ZO1 intensity in the myocardial cells, all images were acquired using the same parameters including laser power, exposure time, and offset settings. The projections of *Z*-stack images were generated; the fluorescence intensity at vertices and edges was measured using Image J. Briefly, maximum projections were obtained from 8-bit *Z*-stack images, which then

were converted into 32-bit images. ‘Threshold’ was applied by using ‘auto’ default settings determined by ImageJ and the background was set to NaN. The regions of ZO1 staining in the vertices (where membranes from three and more adjacent cells contact) and edges (the cell periphery excluding the vertices) were selected, and the mean of the gray value was measured to determine ZO1 intensity.

Supplementary references

Barthel, L. K. and Raymond, P. A. (1990). Improved method for obtaining 3-microns cryosections for immunocytochemistry. *J Histochem Cytochem* **38**, 1383-1388.

Lin, F., Sepich, D. S., Chen, S., Topczewski, J., Yin, C., Solnica-Krezel, L. and Hamm, H. (2005). Essential roles of $Ga_{12/13}$ signaling in distinct cell behaviors driving zebrafish convergence and extension gastrulation movements. *J Cell Biol* **169**, 777-787.

Megason, S. G. (2009). In toto imaging of embryogenesis with confocal time-lapse microscopy. *Meth Mol Biol* **546**, 317-332.

Thisse, C. and Thisse, B. (2008). High-resolution in situ hybridization to whole-mount zebrafish embryos. *Nature Protocols* **3**, 59-69.

Trinh, L. A. and Stainier, D. Y. (2004). Fibronectin regulates epithelial organization during myocardial migration in zebrafish. *Dev Cell* **6**, 371-382.

Ye, D. and Lin, F. (2013). S1pr2/Ga_{13} signaling controls myocardial migration by regulating endoderm convergence. *Development* **140**, 789-799.

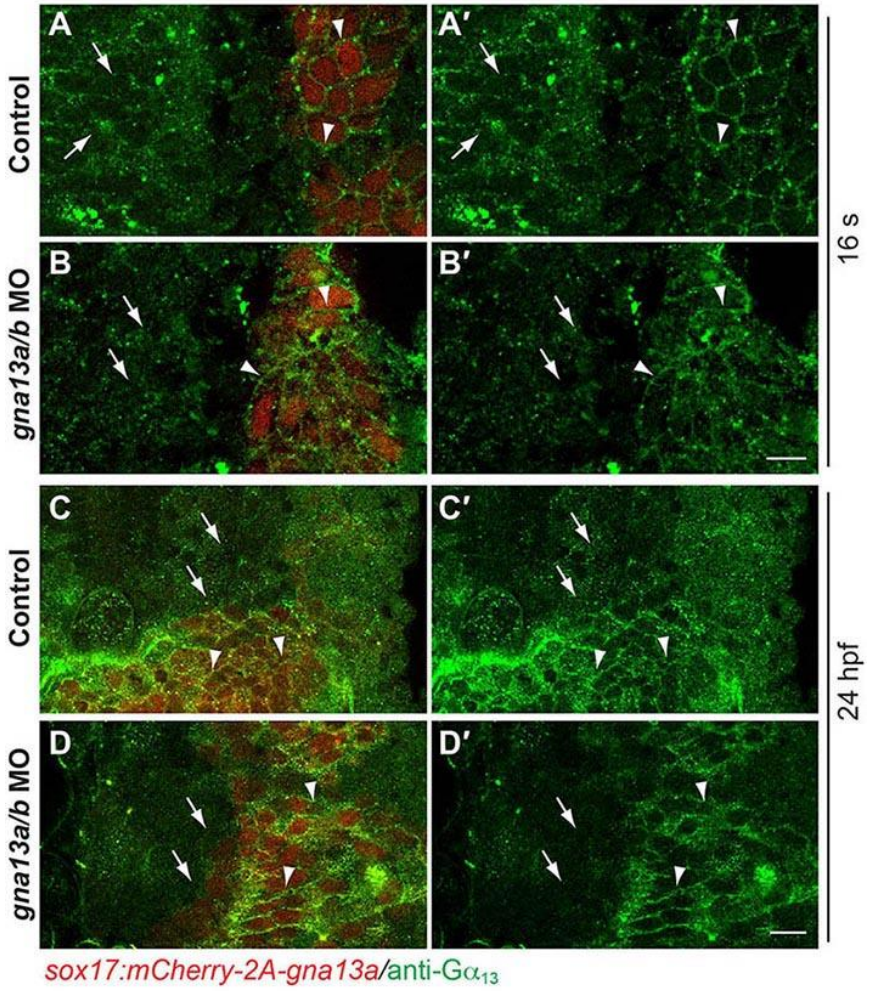

Figure S1. Transgenic Gα$_{13}$ expression in the endoderm is resistant to injection of *gna13a/b* MO. Single confocal Z-planes of the anterior region of embryos in control and *gna13a/b* MO-injected *Tg(sox17:mcherry-2A-gna13a)* embryos at 16s and 24 hpf, showing Gα$_{13}$ expression (green). Arrowheads: endodermal cells (red); arrows: non-endodermal cells. Scale bar: 20 μm.

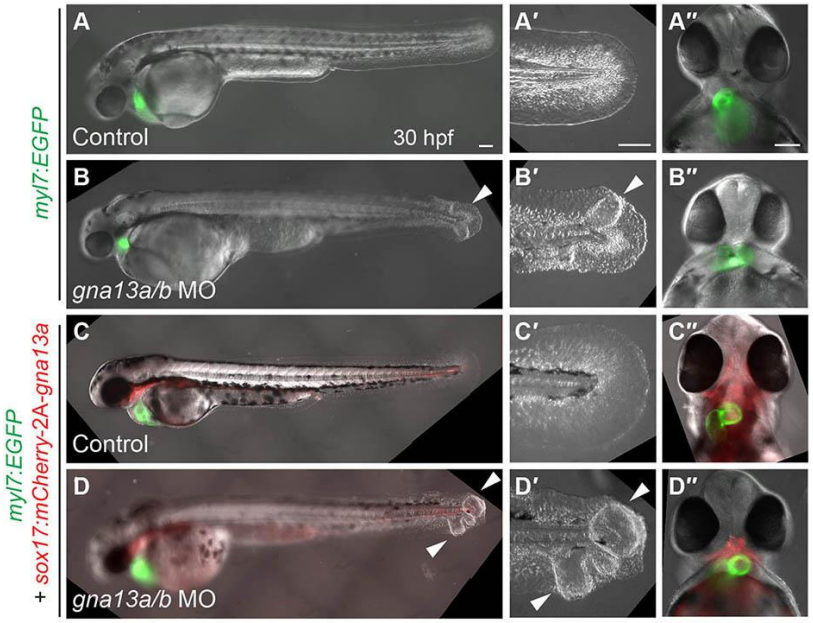

Figure S2. Endodermal Gα$_{13}$ expression rescues cardia bifida, but not tail blistering, caused by Gα$_{13}$ depletion.

(**A-D''**) Overlays of epifluorescence and bright-field images of the indicated embryos at 30 hpf in lateral (A-D') and anterior-ventral (A"-D") views. (A'-D') High-magnification images of the tail region of each embryo. Arrowheads: tail blisters. Scale bar: 100 μm.

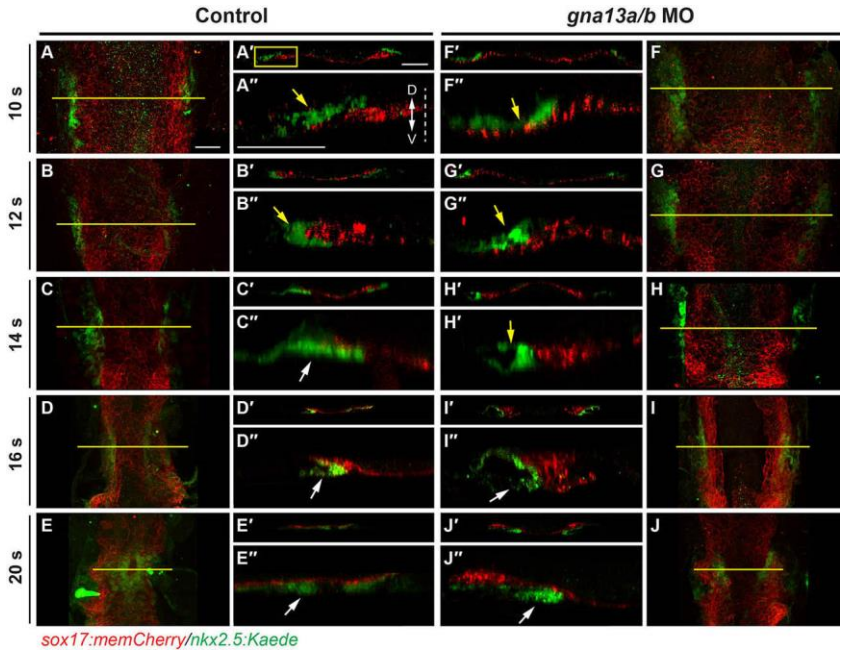

Figure S3. Gα_{13} is required for subduction and the final stage of the medial migration of myocardial precursors.

(**A-J**) Projections of confocal Z-stacks of anterior endoderm and myocardial precursors (taken by a Lan-Apo 20×/NA 0.8 objective) in embryos at different stages as indicated, showing the mCherry-labeled endoderm (red) and Kaede-labeled myocardial cells (green). (**A'-J'**) Images of XZ transverse sections in the areas, as indicated by yellow lines in A-J. (**A"-J"**) Magnified areas of the left region of the XZ transverse sections in A'-J'. Example of region used is indicated by box in A'. Dashed line: midline; arrows: myocardial cells, located above (yellow) and below (white) the endoderm; D: dorsal; V: ventral. Scale bars: 20 μm.

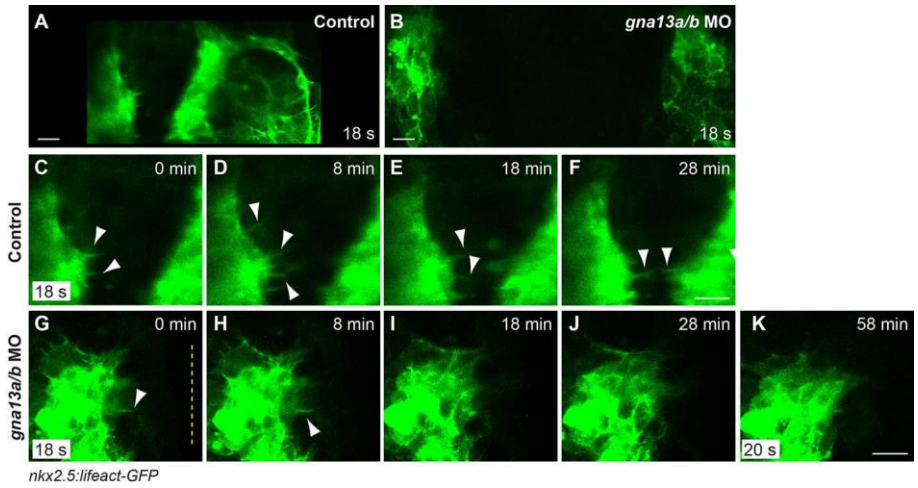

Figure S4. Myocardial precursors form robust migratory protrusions, which are transient in Gα_{13}-deficient embryos.

Snapshots from confocal movies of control and *gna13a/b* MO-injected *Tg(nkx2.5:lifeact-GFP)* embryos (supplementary movie 3). (**A,B**) The myocardial cells at 18s when the time-lapse started. (**C-K**) Magnified images in A-B at the indicated time-points. (C-F) The most dorsal regions of two myocardial populations in control embryos. (G-K) The left side of myocardial populations in morphants. The protrusions were presented initially, but disappeared in morphants. White arrowheads: protrusions. Yellow dashed line: midline. Scale bars: 20 μm.

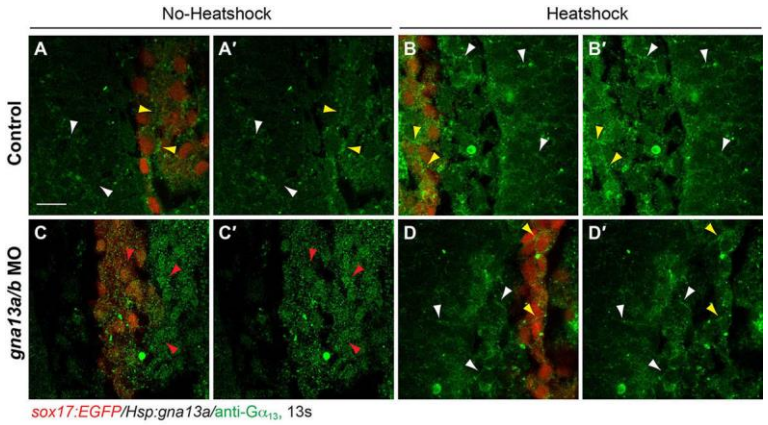

Figure S5. Gα$_{13}$ expression in *Tg(hsp:gna13a)* embryos.

Single confocal Z-planes of the anterior region of embryos obtained from crossing *Tg(sox17:EGFP)* with *Tg(hsp:gna13a)*, showing Gα$_{13}$ expression in non-endodermal cells (white arrowheads) and endodermal cells (yellow arrowheads, false red colored) in indicated embryos that were heat-shocked at 37°C for 30 minutes or left untreated in the tail-bud stage. Gα$_{13}$ expression disappeared in *gna13a/b* MO-injected embryos without heat-shock (red arrowheads). Scale bar: 20 μm.

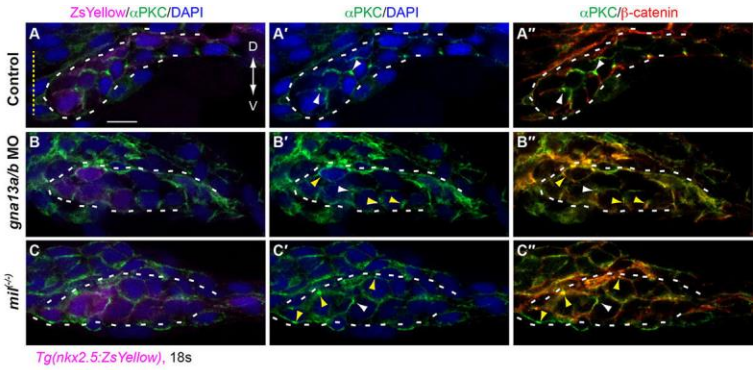

Figure S6. Epithelial organization of myocardial cells is disrupted in Gα_{13} morphants.

Transverse vibratome sections immunostained with ZsYellow (Magenta), αPKC (green), β-catenin (red) and nuclei (DAPI, blue) in control (A), *gna13a/b* MO-injected (B) and *mil* mutant (C) *Tg(nkx2.5:ZsYellow)* embryos at 18s. Yellow dashed line: midline; white dashed lines outline myocardial cells; white arrowheads: normal αPKC expression; yellow arrowheads: ectopic αPKC expression. D: dorsal; V: ventral.

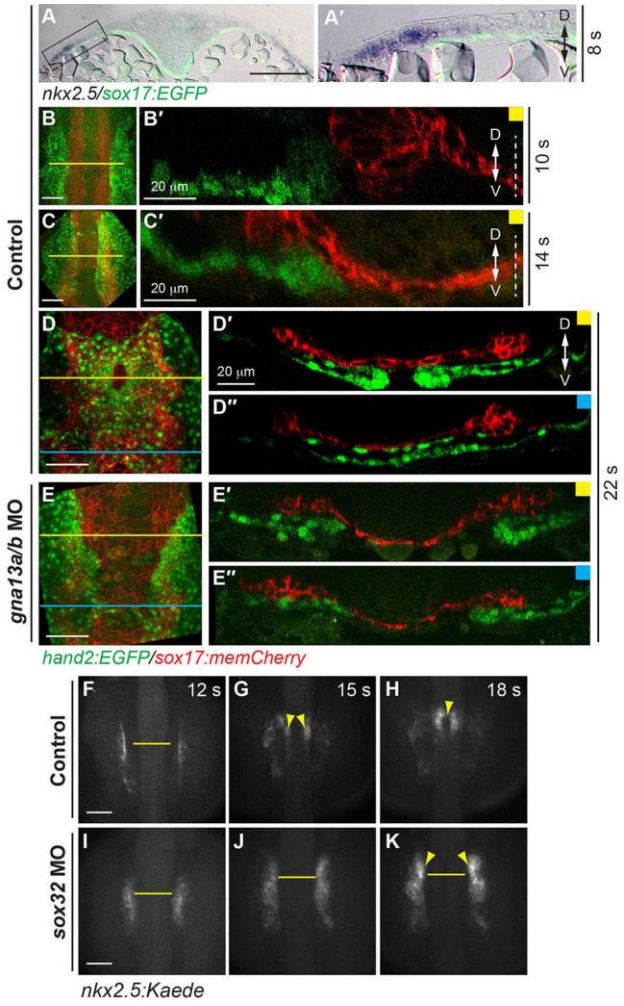

Figure S7. The ALPM engages in subduction, with some cells migrating from the dorsal to the ventral side of the endoderm.

(**A**) The relative positions of the ALPM and endoderm. (A-A') Overlays of GFP (endoderm) and *hand 2* expression as detected by ISH in *Tg*(*sox17:EGFP)* embryos at 8s. (A'): high-magnification image of area indicated in A. (**B**-**E''**) Confocal images of control and *gna13a/b* MO-injected *Tg(hand2:EGFP)/Tg(sox17:memCherry)* embryos at the indicated stages, showing the EGFP-expressing ALPM and memCherry-expressing endoderm. (B-E) Z-projections. Horizontal lines: positions of the XZ sections. (B'-E") XZ views of z-stacks of embryos at positions indicated in B-E. White dashed lines: midline. D: dorsal; V: ventral. (**F**-**K**) Snapshots of myocardial precursors from epifluorescence time-lapse movies taken of control (F-H) or *sox32* MO-injected (I-K) *Tg(nkx2.5:Kaede)* embryos at the indicated stages, using a 5×/NA 0.15 objective. Yellow arrowheads: myocardial cells; yellow lines: the distance between the two populations of myocardial cells (equivalent length). Scale bars: 100 μm, unless stated otherwise.

Movie 1. S1pr2 signaling is required for efficient endoderm convergence during segmentation.

Time-lapse experiments were performed on *Tg(sox17:EGFP)* control or *s1pr2/mil* mutant embryos from 8-20s, using an epifluorescence microscope (DMI 6000, Leica) with a 5×/NA 0.15 objective. Images were captured at 5-minute intervals, and the movie plays at 7 frames/second.

Movie 2. Myocardial migration at all stages is disrupted in $G\alpha_{13}$ morphants.

Time-lapse experiments were performed on control or *gna13a/b* MO-injected *Tg(sox17:memCherry)/(nkx2.5:ZsYellow)* embryos from 9-18 s, using a 10×/NA 0.3 objective, as described for Movie 1. The movie plays at 7 frames/second.

Movie 3. Migratory protrusions of the myocardial cells in control embryos and morphants.

Confocal time-lapse experiments were performed on *Tg(nkx2.5:lifeactGFP)* from 18-22 s, using a Zeiss LSM700 confocal microscope with a Lan-Apo 20×/NA 0.8. Images were captured at 35-second intervals, and the movie plays at 10 frames/second.

Movie 4. Endodermal expression of Gα$_{13}$ rescue defects of endoderm convergence and myocardial migration.

Time-lapse experiments were performed on *Tg(sox17:memCherry)/Tg(nkx2.5:ZsYellow)* or *Tg(sox17:memCherry-2A-gna13a)/Tg(nkx2.5:ZsYellow)* embryos that were injected with *gna13a/b* MO from 9-21 s, using a 10×/NA 0.3 objective, as described for Movie 1. The movie plays at 7 frames/second.

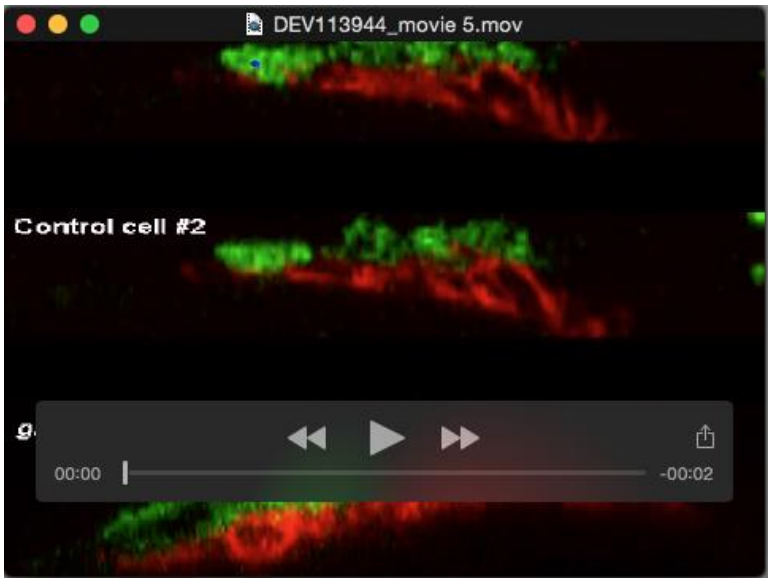

Movie 5. Gα_{13}-mediated endoderm convergence impairs subduction of myocardial precursors.

In toto confocal time-lapse movies were performed on control and *gna13a/b* MO-injected *Tg(sox17:memCherry)/(nkx2.5:Kaede)* embryos from 10-14 s, using a Zeiss LSM700 confocal microscope with a LD C-Apo 40×/NA 1.1 water objective. Images were captured at 5-minute intervals, and the movie plays at 7 frames/second.

Movie 6. The medial movement of ALPM is impaired in Gα_{13} morphants.

Epifluorescence time-lapse experiments were performed on control or *gna13a/b* MO-injected *Tg(sox17:memCherry)/Tg(hand2:EGFP)* embryos from 10-20 s, using a 10×/NA 0.3 objective, as described for Movie 1. Images were captured at 5-minute intervals, and the movie plays at 7 frames/second.

Movie 7. Myocadial cells fail to undergo subduction and medial migration in the absence of endoderm.

Epifluorescence time-lapse experiments were performed on control or *sox32* MO-injected *Tg(nkx2.5:Kaede)* embryos from 10-24 s, using a 5×/NA 0.15 objective, as described for Movie 1. Images were captured at 5-minute intervals, and the movie plays at 7 frames/second.